*J. Fluid Mech.* (1987), *vol.* 179, *pp.* 41–57
*Printed in Great Britain*



# A wake source model for airfoils with separated flow

By G. V. PARKINSON AND W. YEUNG
Department of Mechanical Engineering, The University of British Columbia, 2324 Main Mall, Vancouver, BC, V6T 1W5, Canada

(Received 10 May 1986)

In an extension of an earlier potential-flow theory using conformal mapping and source singularities in the wake region to simulate two-dimensional bluff-body flow, new mapping sequences and additional boundary conditions are presented for the application of the method to lifting airfoils fitted with upper-surface spoilers or lower-surface split flaps of arbitrary size, location, and erection angle. The only empirical input is the base pressure coefficient. Calculations are presented of pressure distribution and lift for several cases of a Joukowsky airfoil fitted with a spoiler or a split flap, and these results are compared with experimental data from wind tunnel tests. Good agreement is found.

## 1. Introduction

The important applied fluid mechanics problem of determining the loading on bodies immersed in a flow can be solved for streamline bodies by a combination of an outer potential-flow model and an inner boundary-layer-flow model. The potential flow alone gives a fairly good estimate of the body pressure distribution, and the combination, using iterative methods, leads to an accurate calculation of both pressure and shear-stress distributions. For bluff bodies, however, the situation is less satisfactory for two reasons. The first is the inability to deal with the interior of the broad wake, usually turbulent for problems of engineering interest and containing organized vortex systems. The second is the uncertainty about wake boundary conditions even if the interior is ignored.

However, since the wake total head is greatly reduced, the body surface exposed to the wake experiences very small shear stresses and a nearly constant time-averaged pressure distribution. This suggests that a potential-flow model could give a satisfactory prediction of pressure loading on a body if the pressure were given correctly at the separation points. Of course, a successful model requires a reasonable simulation of the wake boundary conditions but, since these cannot in any case be precisely defined, 'reasonable' may involve no more than having the streamline simulating the separating shear layer start out in the correct direction with the correct velocity and asymptotically approach the free-stream velocity downstream.

Two-dimensional incompressible flow models using wake singularities at or near the body surface can achieve this degree of wake-boundary simulation, and such models have the advantage that they involve relatively simple conformal mapping methods leading to simple flow solutions since the mapping problem is only for the wetted surface of the body. A model of this kind proposed by Parkinson & Jandali (1970, hereinafter referred to as PJ) was shown to give good estimates of the pressure distribution on several symmetrical bluff sections, and an extension of the model to

lifting airfoil sections with normal spoilers (Jandali & Parkinson 1970, hereinafter referred to as JP), gave similarly good results. In this model the contour to be mapped is the wetted surface plus an additional contour in the wake providing a slit or cusp at each flow separation point. The part of the original contour exposed to the wake is ignored unless it already conforms to the above requirement. Thus, a circular cylinder is treated as a circular-arc slit, and for the airfoil the spoiler is already a slit, while the trailing edge, if not already a cusp, is converted to one. The resulting contour is then mapped to a circle by a set of transformations for which the overall derivative of the mapping function has simple zeros at the flow separation points. In the transform plane the flow model consists of uniform flow plus a doublet for the basic circle, two sources on the wake portion of the contour and their image sink at the centre, and a vortex at the centre for the circulation in lifting configurations. The source and vortex strengths and the source angular positions are five unknowns and four of these are determined by conditions at separation. Two conditions are that the separation points in the physical plane become flow stagnation points in the transform plane, thus ensuring tangential separation of the physical streamlines, since angles are doubled there. The other two conditions are the specification of the velocity at the separation points, given by the base pressure on the body, empirically determined as in all such flow models.

For bluff sections with a continuously curved contour, so that flow separation is boundary-layer controlled, the position of the separation points is also specified empirically in the original model, while for the lifting airfoils the number of unknowns to be solved for is kept at four by arbitrarily locating one of the two wake sources close to the transform stagnation point corresponding to the airfoil trailing edge, investigation having shown the result to be relatively insensitive to this source location. Although the model successfully predicts pressure distributions on a wide variety of sectional shapes, it would clearly be desirable to reduce the empiricism involved, and for the airfoil sections it would be useful to extend the applications from normal spoilers to the more relevant cases of inclined spoilers and split flaps. These possibilities are considered in the present paper.

It has been shown by Woods (1961) that the curvature of the boundary streamline at separation is in general positive infinite or negative infinite, with a single intermediate special case of finite curvature. Negative infinite curvature is possible only for separation at a sharp edge, and if the curvature is positive infinite, so is the streamwise pressure gradient. Therefore, the occurrence of the special finite curvature at separation would appear to be the most natural possibility, and this can be used in the wake source model to eliminate the empirical specification of the separation point. As mentioned in PJ this was tried unsuccessfully for the case of laminar separation from the circular cylinder. More data are now available for the case of turbulent separation from experiments on a circular cylinder by Nakamura & Tomonari (1982), and figure 1 shows a comparison of their data with a theoretical curve for the wake source model using the criterion of finite curvature at separation. (This criterion links the separation angle $\beta_s$ to the base pressure coefficient $C_{pb}$, still given empirically.) The agreement is seen to be quite good, although the experimental pressure gradient is more positive than the finite theoretical gradient prior to separation. Nevertheless, it appears that the criterion can lead to realistic results from the model. Further, the criterion suggests an additional boundary condition for those lifting-airfoil cases with separation in which the separating streamline has naturally positive curvature, e.g. the case of airfoil stall or the flow at the trailing edge of an

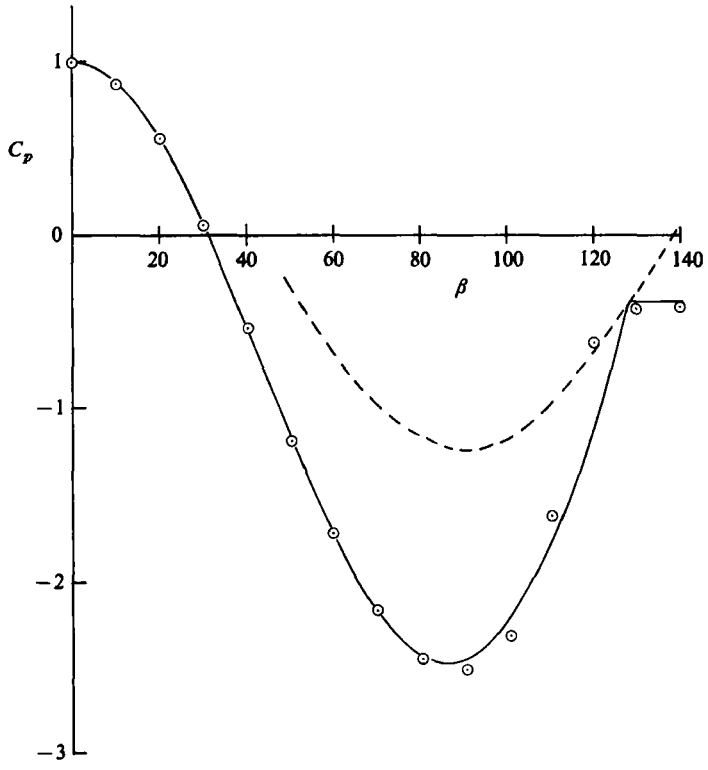


FIGURE 1. Criterion of finite curvature at separation for circular cylinder. ——, theory; – – – –, locus; $C_{pb} = 1 - \frac{9}{4}\sin^2\beta_s$; ○, Nakamura & Tomonari (1982) experiments; Reynolds number $1.7 \times 10^6$.

airfoil with split flap. This idea is explored and applied to extensions of the model in which new mappings permit the consideration of inclined spoilers or split flaps, in addition to the normal spoilers of the original model. Finally, modifications of the use of vortex singularities to satisfy the circulation requirement are considered. Predictions from the new models are compared with experimental data. A more detailed account of the applications is given in Yeung (1985).

## 2. Transformations

In this section the sequence of conformal transformations is described by which the field outside an airfoil of Joukowsky profile with an upper-surface spoiler of arbitrary size, inclination to the surface, and chordwise location is mapped into the field outside the unit circle. The sequence, omitting translations, rotations, and scalings, is shown in figure 2. Minor modifications to this sequence are required to accommodate the configurations of Joukowsky airfoils with lower-surface split flaps. The modification to accommodate a single-element airfoil of arbitrary profile is mentioned later in this section.

The key configuration in the mapping sequence is shown in one of the intermediate transform planes, the $s$-plane of figure 2, a circle with a flat fence at angle $\delta$ to its surface. Proceeding back in the sequence, a translation and rotation to a $t$-plane (not

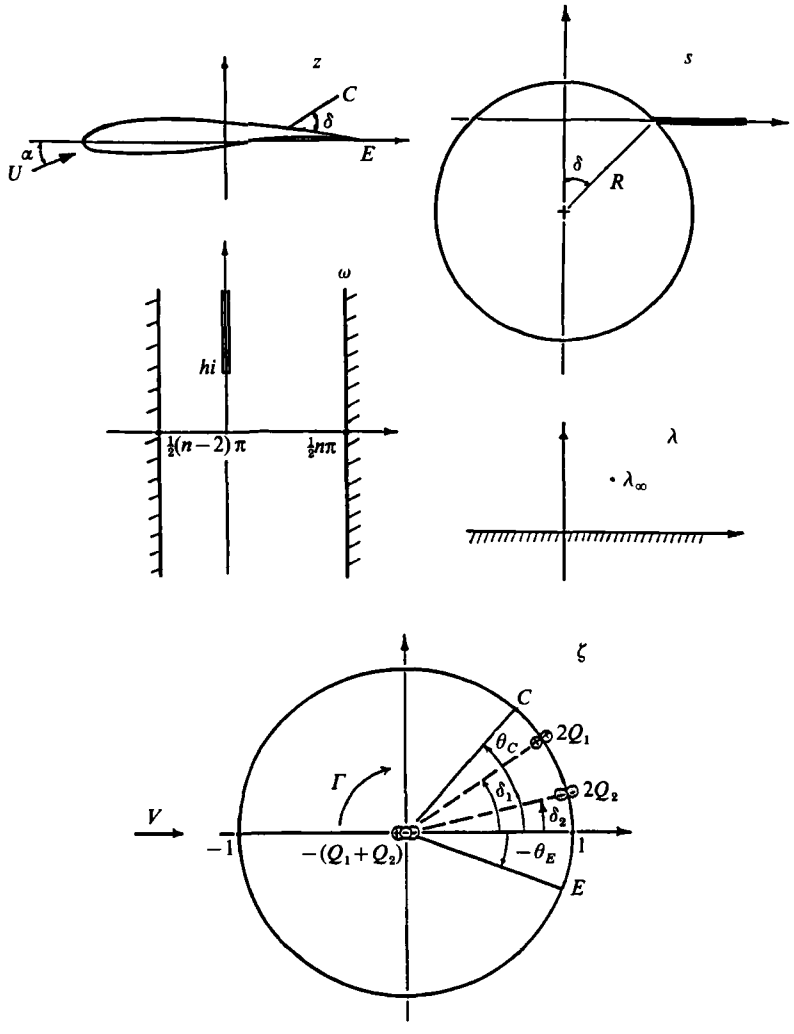


FIGURE 2. Physical and transform planes for Joukowsky airfoil with spoiler.

shown) puts the centre of the circle in the second quadrant and the fence in the first quadrant, while the circle passes through $t = 1$. The Joukowsky transformation,

$$z = t + \frac{1}{t} \tag{2.1}$$

then maps the circle with fence into a thick, cambered Joukowsky-airfoil profile with upper-surface spoiler at angle $\delta$ to the surface. In the transformation from $s$ to $t$ the translation (and the original choice of the radius $R$ of the circle) determine the camber and thickness of the airfoil profile, the rotation determines the chordwise position of the spoiler, and the length of the fence determines the spoiler size.

Proceeding forward from the $s$-plane in the sequence of transformations, use is made of the fact that the circle and fence are on coordinate curves in a bipolar coordinate system. The field exterior to the circle and fence can therefore be mapped to the interior of an infinite strip of the $\omega$-plane, with a slit along the imaginary axis, as shown in figure 2, by the Kármán–Trefftz transformation

$$s = \mathrm{i}R \sin\delta \cot\tfrac{1}{2}\omega. \tag{2.2}$$

The segments of the circle above and below the real axis in the $s$-plane map into the right and left boundaries of the infinite strip, and the fence maps into the slit. The point at infinity in the $s$-plane (and in the physical $z$-plane) becomes the origin in the $\omega$-plane. The infinite strip with slit can be regarded as the interior of a degenerate polygon, a suitable subject for a Schwarz-Christoffel transformation to the upper half $\lambda$-plane, as shown in figure 2 for the choice of boundary points leading to the transformation equation

$$\omega = -\tfrac{1}{2}\pi(2-n)+\mathrm{i}h-\tfrac{1}{2}\mathrm{i}\left[n\ln\left(\frac{\lambda}{n}+1\right)+(2-n)\ln\left(\frac{\lambda}{2-n}-1\right)\right], \tag{2.3}$$

where $n$ and $h$ are defined in the $\omega$-plane. The point $\lambda_\infty$ now represents the point at infinity in the $z$-plane. By a translation and scaling transformation to the $\mu$-plane (not shown), $\lambda_\infty$ is mapped onto $\mu = \mathrm{i}$.

Finally, a bilinear transformation and a rotation,

$$\zeta = \mathrm{e}^{-\mathrm{i}\alpha_0}\left(\frac{\mathrm{i}+\mu}{\mathrm{i}-\mu}\right), \tag{2.4}$$

map the upper half $\mu$-plane onto the exterior of the unit circle in the $\zeta$-plane, with the point at infinity now preserved in the overall transformation from the $z$-plane to the $\zeta$-plane. The purpose of the rotation is to orient the flow at infinity in the $\zeta$-plane in the direction of the real axis, as shown in figure 2. The angle $\alpha_0$ in (2.4) is determined by the angle of attack $\alpha$ of the airfoil in the $z$-plane, and by geometric parameters of the intermediate transformations.

Only the Joukowsky-airfoil profile is studied in this paper. However, the theory can be applied to any single-element-airfoil profile by employing the method of Theodorsen (1931) to map the airfoil profile into a circle. In this application of Theodorsen's method the airfoil with spoiler would be suitably placed in the $z$-plane so that a Joukowsky transformation would map it into a near-circle with fence. The Theodorsen series transformation would then be used to map the near-circle with fence into a true circle with fence, chosen to be flat. This true-circle plane corresponds to the $t$-plane of the basic sequence, and all subsequent transformations leading to the $\zeta$-plane are the same.

The transformation sequences for both the Joukowsky profile and the arbitrary profile satisfy the fundamental requirement of the wake source model that the overall derivative $\mathrm{d}z/\mathrm{d}\zeta$ has simple zeros at the points corresponding to the flow separation points, here the spoiler tip and airfoil trailing edge. In addition, as mentioned in §1, the body profile must have a slit or cusp at the separation points. For the Joukowsky profile, since the spoiler is a slit and the airfoil trailing edge is a cusp, this requirement is satisfied automatically. However, airfoils of arbitrary profile generally have finite trailing-edge angles. In such cases the upper surface of the airfoil (the part exposed to the wake and therefore not of interest in the flow problem) is modified to make the trailing edge a cusp.

## 3. Flow model

### 3.1. *Field equations*

The flow problem is solved in the $\zeta$-plane, and the equations of this section apply to all airfoil configurations considered in the paper. By the transformations of §2 the problem has been reduced to finding the flow, with uniform velocity $V$ in the direction of the real axis at infinity, past a circular cylinder of unit radius centred at the origin,

as shown in figure 2. There is a circulation about the cylinder and the points corresponding to the two separation points on the airfoil are stagnation points of the cylinder flow. These requirements are satisfied by adding to the familiar basic flow (uniform flow + doublet at origin + vortex of strength $\Gamma$ at origin) two sources of strengths $2Q_1$, $2Q_2$ on the portion of the cylinder surface downstream of the specified stagnation points. To satisfy the cylinder boundary condition, that its contour is a streamline of the flow, image sinks of strengths $Q_1$, $Q_2$ are then added at the origin. This leads to a complex velocity given by

$$w(\zeta) = \frac{\mathrm{d}F}{\mathrm{d}\zeta} = V\left(1-\frac{1}{\zeta^2}\right)+\frac{\mathrm{i}\Gamma}{2\pi\zeta}+\frac{Q_1}{\pi}\frac{1}{(\zeta-\mathrm{e}^{\mathrm{i}\delta_1})}+\frac{Q_2}{\pi}\frac{1}{(\zeta-\mathrm{e}^{\mathrm{i}\delta_2})}-\frac{(Q_1+Q_2)}{2\pi\zeta}, \tag{3.1}$$

where $F$ is the complex potential, and angles $\delta_1$ and $\delta_2$ are defined in figure 2. If complex potentials are equated at corresponding points in the $\zeta$- and $z$-planes, then the contour of the airfoil and spoiler is a streamline of the flow in the $z$-plane, and its complex velocity is given by

$$w(z) = \frac{w(\zeta)}{\mathrm{d}z/\mathrm{d}\zeta}. \tag{3.2}$$

As $z$, $\zeta \to \infty$, $w(z) \to U\mathrm{e}^{-\mathrm{i}\alpha}$ and $w(\zeta) \to V$, which can therefore be determined as a function of $U$ and geometric parameters of the transformations by calculating $|\mathrm{d}z/\mathrm{d}\zeta|_{z\to\infty}$.

### 3.2. *Boundary conditions*

The flow model given by (3.1) and (3.2) automatically satisfies the boundary conditions on $w(z)$ of uniform flow at infinity and tangent flow over the body surface. However, (3.1) contains the five unknown parameters $Q_1$, $Q_2$, $\delta_1$, $\delta_2$, and $\Gamma$, requiring five additional boundary conditions. As mentioned in §1, two of these are supplied by the basic requirement that the flow separation points in the $z$-plane must become flow stagnation points in the $\zeta$-plane (points $C$ and $E$ in both planes in figure 2).

$$w(\zeta)\,|_C = w(\zeta)|_E = 0. \tag{3.3}$$

Then, since $C$ and $E$ are critical points of the overall transformation, angles are doubled there in the $z$-plane and the separating streamlines leave the airfoil surface tangentially at the spoiler tip and airfoil trailing edge. Two more boundary conditions are supplied through the empirical assumption of a constant base pressure coefficient $C_{p\mathrm{b}}$ over the portion of the airfoil and spoiler surface exposed to the wake in the real flow. In the flow model this leads to the specification of the separation velocity at $C$ and $E$ in the $z$-plane, through Bernoulli's equation:

$$\left|\frac{w(z)}{U}\right|_C = \left|\frac{w(z)}{U}\right|_E = (1-C_{p\mathrm{b}})^{\frac{1}{2}}. \tag{3.4}$$

In the mathematical model the flow in the wake region inside the separating streamlines, which simulate the shear layers of the real flow, is of no interest and is ignored, except for its influence on the outer flow as discussed later. The use of L'Hôpital's rule for indeterminate forms is needed to evaluate the boundary conditions given by (3,4), since both $w(\zeta)$ and $\mathrm{d}z/\mathrm{d}\zeta$ in (3.2) are zero at points $C$ and $E$.

Thus, four of the unknown parameters are determined by (3.3) and (3.4), and in the original version of the airfoil model (JP) these were chosen to be $Q_1$, $Q_2$, $\delta_1$, and $\Gamma$, while the fifth unknown $\delta_2$ was dealt with by empirically placing the source close

to $E$ in the $\zeta$-plane, as mentioned in §1. This gives satisfactory results, since $Q_2 \to 0$ as the source approaches $E$, and so the aerodynamic loading on the airfoil is relatively insensitive to the exact value of $\delta_2$. However, the additional empiricism is undesirable, and so for the new version of the model an effort was made to devise a fifth boundary condition with a reasonable physical basis. It should be mentioned that one alternative suggestion was to regard the vortex as an unnecessary addition to the flow model and thus eliminate $\Gamma$, leaving only four unknowns to satisfy the four boundary conditions, as in the original wake-source model for non-lifting bodies (PJ). However, this failed completely to produce realistic results for airfoils with spoilers or split flaps.

Therefore, $\Gamma$ is needed to determine the airfoil circulation, and it is reasonable to assume that the fifth boundary condition should be related to the circulation. In the real flow, the wake region makes no contribution to the time-averaged airfoil circulation, which is therefore a consequence of the unseparated flow upstream of the spoiler tip and airfoil trailing edge. If, then, in the flow model the wake region is also required to make no contribution to the airfoil circulation, the upstream flow should be a better simulation of the real flow. Thus, a suitable fifth boundary condition is

$$\Gamma_w = \mathrm{Re} \int_w w(z)\,\mathrm{d}z = \mathrm{Re} \int_w w(\zeta)\,\mathrm{d}\zeta = 0, \tag{3.5}$$

where the integral is over the portion of the contour exposed to the wake in the $z$-plane or, more usefully, in the $\zeta$-plane, since the integral is preserved in the transformation. The combination of (3.3), (3.4), and (3.5) gives five equations for the five unknown constants, and will be shown later to give good results for airfoils with spoilers (these remarks also apply to split flaps) located relatively near the airfoil trailing edge and with $\delta \leqslant 45°$. However, if the spoiler is too far forward or if $\delta$ is too large, the equations cannot be satisfied unless the empirical value of $C_{pb}$ is adjusted. This can still lead to a satisfactory simulation of the airfoil pressure distribution except near the separation points, but it would of course be desirable to use the true experimental value of $C_{pb}$, rather than an adjusted value, in all cases. The second author has proposed a procedure which achieves this objective as follows.

In the previous spoiler paper (JP), in addition to the version of the flow model described earlier in this section, a simpler version called the one-source model was also presented. In it one source is eliminated, so that $Q_2 = \delta_2 = 0$ and only the three unknowns $Q_1$, $\delta_1$, $\Gamma$ remain to be determined by the two equations (3.3) and one of (3.4). In this way tangential flow at separation is achieved, but at the correct velocity at only one of the separation points, so that there is in general a pressure discontinuity at the other one. However, the simulation of the complete airfoil pressure distribution is quite good, and if the one-source model equations are solved twice for a given airfoil-spoiler configuration, with (3.4) satisfied first at the spoiler tip and then at the airfoil trailing edge, the two theoretical curves of pressure distribution typically bracket the experimental points closely. In the proposed procedure the integral $\Gamma_w$ of (3.5) is evaluated with the integrand $w(\zeta)$ supplied by a solution of the one-source model. Instead of zero, values $\Gamma_{w1}$ and $\Gamma_{w2}$ are obtained from the two possible one-source solutions for a given airfoil-spoiler configuration. Then, for the fifth boundary condition in the original problem of the two-source model, (3.5) is replaced by

$$\Gamma_w = \mathrm{Re} \int_w w(\zeta)\mathrm{d}\zeta = \tfrac{1}{2}(\Gamma_{w1} + \Gamma_{w2}). \tag{3.6}$$

In (3.6), the right-hand side is not necessarily zero, but in view of the behaviour of the one-source model solutions it is expected that (3.6) will ensure a flow outside the wake region that closely simulates the real flow. The procedure is akin to an iterative method. In test applications to airfoil-spoiler and airfoil-split-flap configurations, it has always proved possible to satisfy the set of five boundary conditions given by (3.3), (3.4) and (3.6) with only the experimental value of $C_{pb}$ as an empirical input, so as a result this procedure has been adopted as standard. The result of course is not the solution of a complete boundary-value problem because the conditions along the free streamlines bounding the wake region are undefined in wake-source models except at separation and at infinity.

### 3.3. *Method of solution*

The simultaneous solution of the five equations (3.3), (3.4), and either (3.5) or (3.6) for the five unknown parameters $\Gamma$, $Q_1$, $Q_2$, $\delta_1$, and $\delta_2$ is complicated by the fact that in all of the equations, while $\Gamma$, $Q_1$, and $Q_2$ enter linearly, angles $\delta_1$ and $\delta_2$ enter nonlinearly, so that a numerical solution is required. Of several procedures tried, the following has been found to be the most satisfactory.

Since for an acceptable solution the sources must be located on the part of the contour exposed to the wake, in figure 2

$$\theta_E < \delta_1, \quad \delta_2 < \theta_C,$$

where $\zeta = e^{i\theta}$ on the circle in the $\zeta$-plane. Therefore, $\delta_2$ is assigned one of a set of values

$$\delta_2 = \theta_E + \frac{(\theta_C - \theta_E)\, m}{n+1} \quad (m = 1,2,\ldots,n), \tag{3.7}$$

and (3.3) and (3.4) are used to solve for the remaining unknowns $\Gamma$, $Q_1$, $Q_2$, $\delta_1$. This is done by successively eliminating the linear parameters $\Gamma$, $Q_1$, $Q_2$, and solving the remaining relation numerically for $\delta_1$. $\Gamma$, $Q_1$, and $Q_2$ are next obtained by substitution. These tentative solutions are then substituted in either (3.5) or (3.6), and will not in general satisfy the equation, so that a residue is left. If so, the next value of $\delta_2$ is assigned from the sequence given by (3.7) and the entire procedure is repeated until the residue is found to vanish or change sign, thus assuring a solution. With the parameters determined, $w(\zeta)$ is given by (3.1), $w(z)$ by (3.2), and the airfoil pressure distribution by Bernoulli's equation

$$C_P = 1 - \left| \frac{w(z)}{U} \right|^2. \tag{3.8}$$

The airfoil lift coefficient $C_L$ is determined by numerical integration of the pressure distribution.

## 4. Experiments

Experiments were performed for two purposes, first, to measure the base pressure values that form the required empirical input to the theory, secondly, to make comparisons between the theoretical and experimental pressure distributions and the overall lift forces on the airfoil at different angles of attack and for the various configurations involved.

Two series of experiments were carried out: one involving the airfoil and spoilers, and the other with the airfoil and split flaps. They were conducted in the small low-speed aeronautical wind tunnel in the Department of Mechanical Engineering at

the University of British Columbia. It has a test section of 27 in. height × 36 in. width. The tunnel possesses good flow uniformity and a turbulence level of less than 0.1 % over its speed range. The Joukowsky airfoil of 27 in. span, 12.08 in. chord, 11 % thickness and 2.4 % camber was mounted vertically, with small clearances at the ceiling and the floor, on a six component pyramidal balance situated beneath the test section of the tunnel.

The airfoil was originally designed for Jandali's experiments on normal upper-surface spoilers, described in (JP), and there is a point worth noting. Since the Joukowsky profile was structurally weak near the cusped trailing edge, the upper surface in this portion was thickened to give an approximately constant thickness of $\frac{1}{8}$ inch. This modified portion does not influence the pressure measurements for the upper-surface spoiler experiments because then it is completely embedded in the wake and has no effect on the outer flow. However, it does lead to some error in pressure measurement near the upper-surface trailing edge in airfoil experiments with lower-surface split flaps. It would have been preferable for the split-flap experiments to have this modified portion located on the lower surface of the airfoil so that it would again be exposed to the wake. Details of the pressure variation along this portion of the upper surface are crucial to the criterion of the finite pressure gradient at separation to be discussed later.

In the experiments, end plates on the airfoil were used to allow the spoiler or split flap to be located at various positions and angles of inclination. The spoilers of height 5 % and 10 % chord could be mounted at distances of 50 %, 70 % and 90 % chord from the leading edge of the airfoil. The 5 % chord spoiler could only be inclined at 45° whereas the 10 % chord spoiler could be deflected at 30° or 60° with respect to the local upper surface of the airfoil. The two split flaps used were of 20 % and 30 % chord, located at their chord distance from the trailing edge. The angles of inclination were 10°, 30°, 45° and 60°. The small gap between the spoiler or flap and the airfoil surface was sealed.

Owing to the small sizes of spoilers used, pressure measurements were made only on the wetted surface of each flap. They were obtained by taping pressure tubing over the surface so that the tubes were exposed to the outer flow. The pressures on the surface of the airfoil, including the portion within the wake, however, were measured by using the pressure taps built into the Joukowsky airfoil. All pressure taps were connected to a 48 port scanivalve, a manually scanning pressure transducer. A Setra 237 differential pressure transducer, a HP 6204B d.c. power supply, a Solartron JM 1860 time domain analyser and a Fluke 8000A digital multimeter were used for data recording. Because of time limitations, no data acquisition system controlled by a microprocessor was set up.

In addition to supporting the airfoil, the balance was used to measure not only the lift, but the drag and pitching moment, needed for the wind-tunnel wall corrections, which were made to the data by standard methods. The corrected $C_P$ values were then integrated to give $C_L$ by using the same numerical integration procedure as for the theoretical distributions. This $C_L$ instead of the one calculated from the balance data will be compared in the next sections to the theoretical predictions. The test Reynolds number was $3 \times 10^5$.

## 5. Results for airfoil with spoiler

Samples of the theoretical and experimental results obtained for the Joukowsky airfoil fitted with different upper-surface spoilers are given in figures 3–7. Boundary

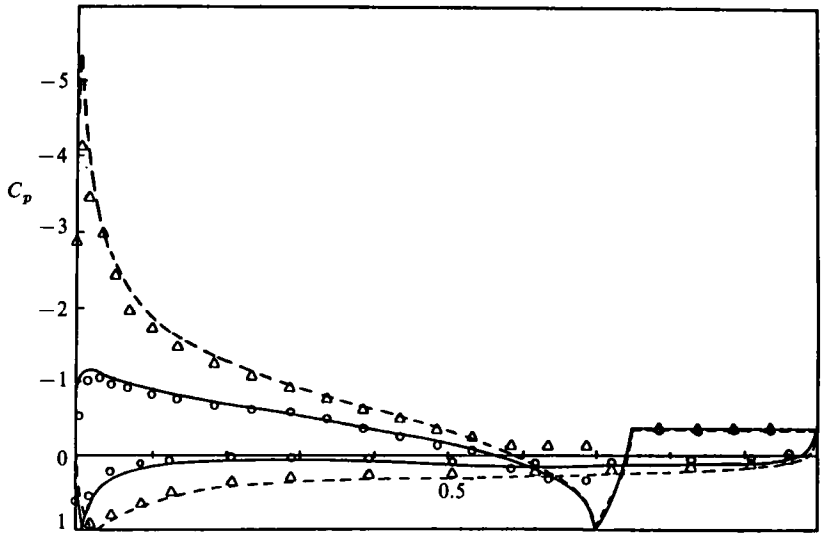


FIGURE 3. Pressure distributions on Joukowsky airfoil with 5 % spoiler at 70 % chord. $\delta = 45°$. ——, theory; ○, experiment: $\alpha = 6°$. – – – –, theory; △, experiment: $\alpha = 12°$.

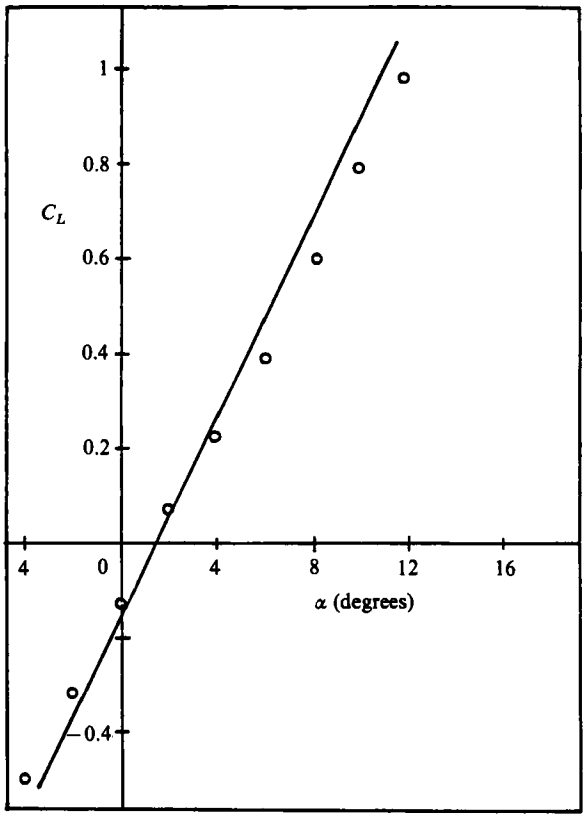


FIGURE 4. Lift *vs.* angle of attack for Joukowsky airfoil with 5 % spoiler at 70 % chord. $\delta = 45°$. ——, theory; ○, experiment.

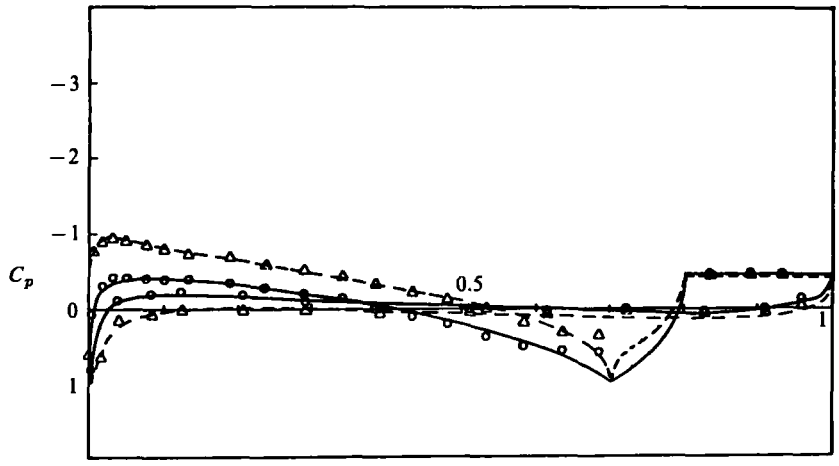


FIGURE 5. Pressure distributions on Joukowsky airfoil with 10% spoiler at 70% chord. $\alpha = 6°$. – – –, theory; △, experiment: $\delta = 30°$. ——, theory; ○, experiment: $\delta = 60°$.

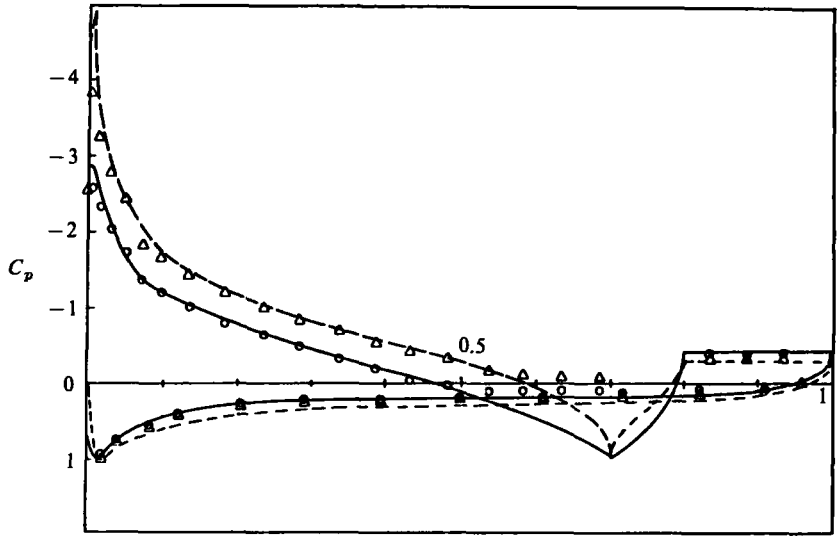


FIGURE 6. Pressure distributions on Joukowsky airfoil with 10% spoiler at 70% chord. $\alpha = 12°$. – – –, theory; △, experiment: $\delta = 30°$. ——, theory; ○, experiment: $\delta = 60°$.

condition (3.6) was used in the theoretical solutions. In figure 3 pressure distributions are shown for the airfoil with a 5% spoiler at 45° located at 70% chord. Theoretical curves are compared with experimental data for two angles of attack, and good agreement is seen in both cases except just upstream of the spoiler, where in the experiments the adverse boundary-layer pressure gradient has produced a constant-pressure separation bubble instead of the potential-flow stagnation-point region. As would be expected, this bubble is larger at $\alpha = 12°$ than at $\alpha = 6°$. In figure 4 theoretical and experimental variations of lift coefficient with angle of attack are compared for the airfoil–spoiler configuration of figure 3. Quite good agreement is seen, with the lower slope of the experimental variation presumably reflecting the

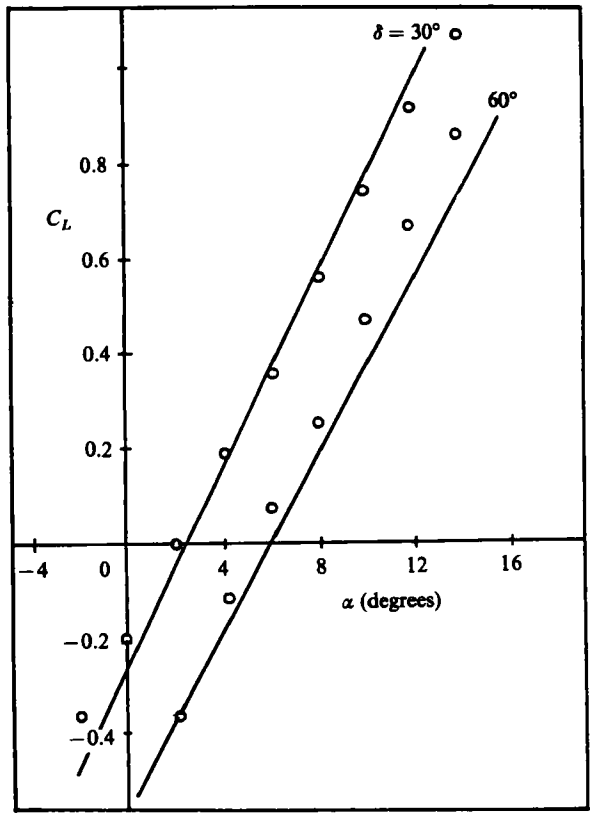


FIGURE 7. Lift *vs.* angle of attack for Joukowsky airfoil with 10% spoiler at 70% chord. ——, theory, ○, experiment.

influence of the boundary layer in reducing the circulation below the potential-flow value.

In figures 5 and 6 pressure distributions are shown for the airfoil with a 10% spoiler located at 70% chord. Comparisons between theoretical and experimental results are given for two spoiler deflections and two angles of attack, and again good agreement is seen except for the presence of the spoiler separation bubbles. In figure 7 the $C_L$-$\alpha$ variations are compared for the configurations of figures 5 and 6. Again theory and experiment are in quite good agreement. A noteworthy feature is that for 60° spoiler deflection the experimental lift exceeded the theoretically predicted values. This appears to be attributable to the considerable lift increment produced by the suction in the relatively large separation bubble resulting from the combination of a large spoiler with a large deflection angle. Results similar to those of figures 3–7 were obtained for other spoiler–airfoil configurations tested.

## 6. Airfoil with split flap

### 6.1. *Modifications to theory*

Split flaps, although not now as widely used on aircraft as spoilers, are still important. Several current designs employ them rather than simple flaps or slotted flaps because of their simplicity and combined high lift and drag characteristics,

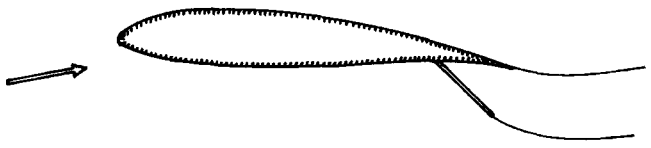

FIGURE 8. Airfoil with split flap.

effective in the landing approach. Since, as can be seen from figure 8, the split flap can be regarded as a spoiler transferred from the airfoil upper surface to the trailing-edge portion of the lower surface, no basic changes are required in the theory for the sequence of conformal transformations or for the flow model. There are some minor changes in the transformation equations arising from the geometric differences in the two systems.

For the flow model, the basic flow in the circle or $\zeta$-plane is again given by (3.1), and the corresponding flow in the airfoil or $z$-plane by (3.2). To determine the unknown parameters in (3.1) the standard method is again to use (3.3), (3.4) and (3.6), with only the experimental value of $C_{pb}$ as an empirical input. Equation (3.5) can be used instead of (3.6) for airfoils with split flaps of 20 % chord or less deflected to 45° or less.

One other boundary condition was tried as an alternative to (3.6) for the airfoil with split flap. The problem of the curvature of the wake boundary streamline at separation from the body was discussed in §1, and it was suggested that the criterion of finite curvature at separation might provide a suitable boundary condition for the upper-surface trailing edge of an airfoil with split flap, where one might expect the streamline curvature to be naturally positive when the airfoil is at a positive angle of attack, as indicated in figure 8. If the streamline curvature is positive and finite at separation, so is the streamwise pressure gradient, and published data for airfoils with split flaps show this to be the case at high angles of attack. It therefore seemed worthwhile to apply this criterion to the potential flow model. Here the streamwise pressure gradient is given in terms of the streamwise velocity gradient through Bernoulli's equation and when this is evaluated at the trailing-edge separation point, using L'Hôpital's rule for the indeterminate forms, the resulting equation is

$$f_2' f_1'' - f_1' f_2'' = 0, \tag{6.1}$$

where $$f_1 = |w(\zeta)|_E, \quad f_2 = \left|\frac{\mathrm{d}z}{\mathrm{d}\zeta}\right|_E, \quad (\ )' = \frac{\mathrm{d}}{\mathrm{d}\theta}(\ ).$$

### 6.2. *Results and comparisons*

Figure 9 shows pressure distributions for the Joukowsky airfoil with the 20 % chord split flap deflected 30°, and the airfoil at 4° angle of attack. Two theoretical curves, calculated using (3.5) and (6.1) respectively as the fifth boundary condition, are compared with experimental data. Both theoretical models are seen to give good agreement with the data, with the main differences occurring at the trailing edge. The model using (3.5) ($\Gamma_w = 0$) predicts a negative infinite pressure gradient at the airfoil and flap trailing edges, whereas a solution was obtained using (6.1) (finite streamline curvature and pressure gradient at trailing edge) only by allowing a less negative $C_{pb}$ than the experimental value of $-0.55$. In our experiment the actual pressure gradient at the airfoil upper-surface trailing edge could not be determined because of the previously-mentioned artificial thickening there, and because there

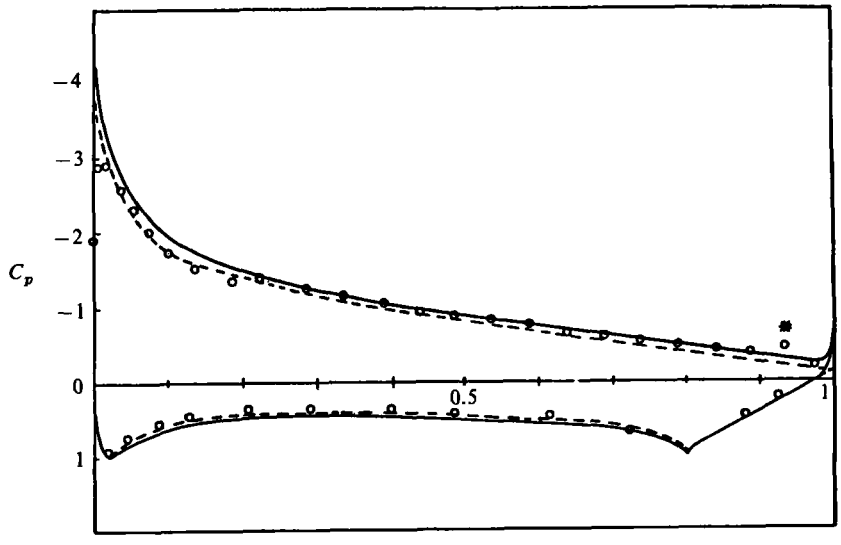


FIGURE 9. Pressure distributions on Joukowsky airfoil with 20 % split flap. $\delta = 30°$. $\alpha = 4°$. ——, theory with (3.5); – – – –, theory with (6.1); ○, experiment.

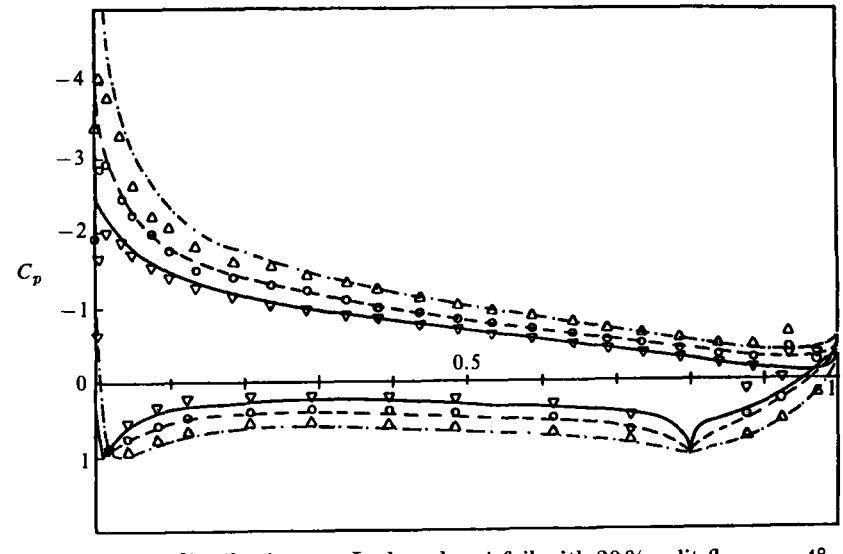


FIGURE 10. Pressure distributions on Joukowsky airfoil with 20 % split flap. $\alpha = 4°$. ——, theory; ▽, experiment: $\delta = 10°$. – – – –, theory; ○, experiment: $\delta = 30°$. —·—, theory; △, experiment: $\delta = 60°$.

were too few pressure taps. The effect of the artificial thickening is seen in figure 9 at the data point marked with a star, representing the last tap on the airfoil upper surface. In published data on pressure distributions for airfoils with split flaps, both conditions occur. An airfoil at low angle of attack may show a negative infinite gradient at the trailing edge, whereas at high angle of attack the corresponding gradient becomes a finite continuation of the upstream gradient, as in the curve in figure 9 calculated using (6.1).

In the remaining results presented, (3.6) was used as the fifth boundary condition,

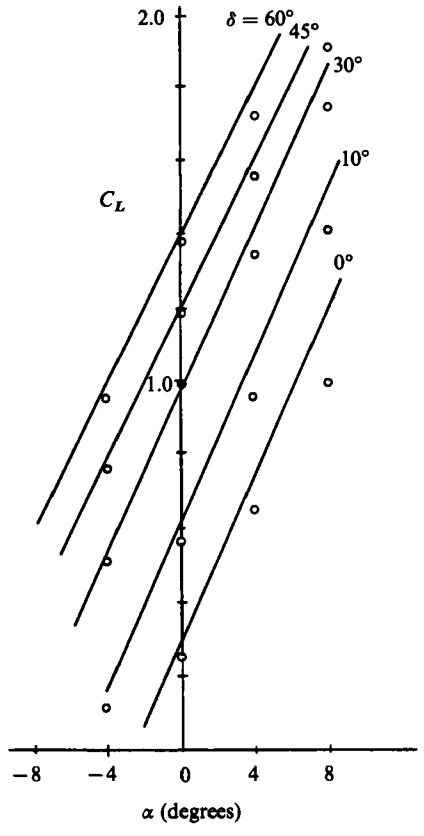


FIGURE 11. Lift *vs.* angle of attack for Joukowsky airfoil with 20% split flap. ——, theory; ○, experiment.

and in all cases it was possible to obtain solutions with the experimental value of $C_{pb}$ as the empirical input. Figure 10 shows comparisons of theoretical and experimental pressure distributions for the Joukowsky airfoil at 4° angle of attack with the 20% chord split flap deflected 10°, 30°, and 60°. For all three cases there is close agreement between theory and experiment, with the following exceptions. As in all the experimental data for the Joukowsky airfoil with split flap, the data point nearest the trailing edge for the upper surface should be disregarded, since it reflects the artificial thickening of that portion. For $\delta = 60°$, the theory overestimates the leading-edge suction peak, presumably because of boundary-layer effects in reducing the circulation. For $\delta = 10°$, the theoretical pressure distribution on the upstream surface of the flap is more positive than the experimental distribution.

In figure 11 the theoretical and experimental $C_L$-$\alpha$ variations are compared for the three configurations of figure 10, plus the basic airfoil ($\delta = 0$) and the case with $\delta = 45°$. Again there is good general agreement, with the expected progressive drop of the experimental values below the theoretical as $\alpha$ increases, because of the boundary-layer effect on airfoil circulation. Results similar to those of figures 9–11 were obtained for other split-flap configurations tested.

## 7. Discussion

The results of figures 3–7 and 9–11 indicate that the wake-source model gives good predictions of pressure distribution and lift on an airfoil with a spoiler or split flap. The model is convenient to use since the flow system given by (3.1) is very simple and the sequence of conformal mappings, while algebraically more complicated than in PJ or JP, is still relatively easy to deal with in calculations.

The separation bubble in front of the control surface is not modelled, but its neglect appears to produce a purely local discrepancy in the pressure distribution for the airfoil with spoiler, and no significant effect at all for the airfoil with split flap.

The model required one empirical input, the experimental value of $C_{pb}$. This is true of all bluff-body potential flow models, and cannot be avoided since $C_{pb}$ is determined mainly by the wake dynamics, which are not modelled. However, two facts diminish the importance of this residual empiricism. First, the experimental variation of $C_{pb}$ is quite small for both spoilers and split flaps, with values generally in the range $-0.6$ to $-0.4$ except at very small values of $\delta$. (Here it should be pointed out that the model may not be applicable to some configurations with spoilers at small deflection angles because of possible flow reattachment near the airfoil trailing edge.) Second, the theoretical airfoil pressure distribution is relatively insensitive to the value of $C_{pb}$ used. This is suggested by figure 9, where although the two theoretical curves are calculated using $C_{pb}$ values of $-0.55$ and $-0.10$ (the experimental value was $-0.55$) both curves give close agreement with the experimental pressure distribution. Further, when the curve satisfying circulation boundary condition (3.5) is calculated for $C_{pb} = -0.45$ and $-0.65$ the results are indistinguishable from the curve plotted in figure 9 except close to the airfoil trailing edge where the values approach $C_{pb}$. Therefore, given an arbitrary configuration of an airfoil with a spoiler or split flap, one might guess at a $C_{pb}$ of, say, $-0.5$ and expect the model to give quite a good prediction of the pressure distribution.

The circulation boundary conditions, (3.5) or (3.6), gave satisfactory results, whereas the finite trailing-edge pressure gradient condition, (6.1), was less satisfactory. Nevertheless, it represents an interesting issue, and deserves further study, since experiments clearly show that it can occur, but only for certain combinations of airfoil-flap configuration and angle of attack. However, it is recommended that circulation condition (3.6) be used as the general fifth boundary condition.

Finally, another possible use of the model is worth mentioning. The sequence of conformal transformations can be modified to provide for tangential streamline separation from any point of the airfoil surface. Using this, perhaps in iterative combination with boundary-layer calculations, one could create a model of airfoil stall. Some preliminary work has been done on this problem.

The experiments on split flaps were carried out by T. Y. Lu. Financial support for the entire study was provided through a grant from the Natural Sciences and Engineering Research Council of Canada.

## REFERENCES

JANDALI, T. & PARKINSON, G. V. 1970 A potential flow theory for airfoil spoilers, *Trans. CASI* **3**, 1.

NAKAMURA, Y. & TOMONARI, Y. 1982 The effects of surface roughness on the flow past circular cylinders at high Reynolds numbers. *J. Fluid Mech.* **123**, 363.

PARKINSON, G. V. & JANDALI, T. 1970 A wake source model for bluff body potential flow. *J. Fluid Mech.* **40**, 577.

THEODORSEN, T. 1931 Theory of wing sections of arbitrary shape. *NACA Rep.* no. 411.

WOODS, L. C. 1961 *The Theory of Subsonic Plane Flow*. Cambridge University Press.

YEUNG, W. 1985 A mathematical model for airfoils with spoilers or split flaps. MASc thesis, University of British Columbia.